Biochemical and Biophysical Research Communications 392 (2010) 106–111

Contents lists available at ScienceDirect

Biochemical and Biophysical Research Communications

journal homepage: www.elsevier.com/locate/ybbrc

Crystal structure of non-redox regulated SSADH from *Escherichia coli*

Jae-Woo Ahn [1], Yeon-Gil Kim [1], Kyung-Jin Kim *

Pohang Accelerator Laboratory, Pohang University of Science and Technology, San31, Hyoja-Dong, Nam-Gu, Pohang, Kyungbuk 790-784, Republic of Korea

ARTICLE INFO

Article history:
Received 2 January 2010
Available online 7 January 2010

Keywords:
SSADH
GABA
Redox-switch modulation
Crystal structure

ABSTRACT

SSADH is involved in the final step of GABA degradation, converting SSA to succinic acid in the human mitochondrial matrix, and its activity is known to be regulated via 'redox-switch modulation' of the catalytic loop. We present the crystal structure of *Ec*SSADH, revealing that the catalytic loop of *Ec*SSADH, unlike that of human SSADH, does not undergo disulfide bond-mediated structural changes upon changes of environmental redox status. Subsequent redox change experiments using recombinant proteins confirm the non-redox regulation of this protein. Detailed structural analysis shows that a difference in the conformation of the connecting loop (β15–β16) causes the formation of a water molecule-mediated hydrogen bond network between the connecting loop and the catalytic loop in *Ec*SSADH, making the catalytic loop of *Ec*SSADH more rigid compared to that of human SSADH. The cytosolic localization of *Ec*SSADH and the cellular function of the GABA shunt in *E. coli* might result in the non-redox mediated regulatory mechanisms of the protein.

Introduction

In humans, Succinic semialdehyde dehydrogenase (SSADH) deficiency is a rare autosomal recessive disease caused by an inherited deficiency in the final step of degradation of the inhibitory neurotransmitter γ-aminobutyric acid (GABA) [1,2]. In the "GABA shunt", a metabolic pathway of GABA, GABA is synthesized from glutamic acid by glutamic acid decarboxylase [3,4]. GABA is then converted to succinic semialdehyde (SSA) by GABA transaminase [5–7], and further converted either to succinic acid by SSADH in the mitochondrial matrix or to γ-hydroxybutyric acid (GHB) by the enzyme SSA reductase [8,9]. The carbon skeleton of GABA therefore enters the tricarboxylic acid cycle in the form of succinic acid. Patients with SSADH deficiency display a variable clinical phenotype, including psychomotor retardation, muscular hypotonia, language delay, ataxia and seizures, exhibiting a 30-fold increase of GHB and a 2- to 4-fold increase of GABA in the brain, compared with normal concentrations of these compounds [10]. A murine SSADH-deficient model ($SSADH^{-/-}$ mice) displays a phenotype that is characterized by ataxia and generalized seizures, and shows increased amount of both GABA and GHB in urine, and in homogenates of brain and liver [11–14]. It is also reported that oxidative stress causes tissue damage in the null mouse model [15]. Recently, our group determined the crystal structure of human SSADH, revealing that the protein is regulated via a 'redox-switch modulation' by sensing changes in environmental redox status [16].

In *Escherichia coli*, an SSADH coding gene *gabD* is located in the *gab* operon, which comprises *gabT* (γ-aminobutyrate transferase), *gabD* (SSADH), *gabP* (GABA permease) and *gabC* (a regulatory gene), and the products of the *gab* operon are involved in GABA degradation [17–19]. *E. coli* SSADH (*Ec*SSADH) lacks an N-terminal signal sequences and shares 54% amino acid identity with human SSADH. *Ec*SSADH is located in the cytosol and the GABA shunt functions to utilize GABA as the sole nitrogen source in *E. coli*. Here we performed structural and biochemical studies on *Ec*SSADH to investigate if *Ec*SSADH is also regulated by a 'redox-switch modulation'. In this study, we present a 1.4 Å resolution crystal structure of *Ec*SSADH revealing that the binding modes of SSA and the enzyme reaction mechanism might be similar to those of human SSADH. However, unlike human SSADH, *Ec*SSADH does not undergo disulfide-bond-mediated structural changes upon redox changes in the environment. Redox change experiments using recombinant proteins also confirm that *Ec*SSADH is non-redox regulated.

Materials and methods

Preparation of EcSSADH. The gene coding for full length *Ec*SSADH (1–482) was amplified from the chromosomal DNA of an *E. coli* strain by a polymerase chain reaction (PCR). The PCR product was then subcloned into $pP_{RO}EX$ HTa (Invitrogen) with $^{**}6\times$His at the N-terminus and a recombinant TEV protease (rTEV) cleavage site. The resulting expression vector $pP_{RO}EX$ HTa:*Ecssadh* was

* Corresponding author. Fax: +82 54 279 1599.
E-mail address: kkj@postech.ac.kr (K.-J. Kim).
[1] These authors contributed equally to this work.

0006-291X/$ - see front matter © 2010 Elsevier Inc. All rights reserved.
doi:10.1016/j.bbrc.2010.01.014

transformed into *E. coli* B834 strain and was grown in an LB medium containing 100 μg/ml ampicillin at 37 °C to an OD_{600} of 0.6. After induction with 1.0 mM IPTG for a further 20 h at 22 °C, the culture was harvested by centrifugation at 5000*g* for 15 min at 4 °C. The cell pellet was resuspended in ice-cold buffer A (50 mM Tris–HCl, pH 8.0, 5 mM of β-mercaptoethanol) and disrupted by ultrasonication. Cell debris was removed by centrifugation at 11,000*g* for 1 h, and lysate was bound to Ni–NTA agarose (QIAGEN). After washing with buffer A containing 10 mM imidazole, the bound proteins were eluted with 300 mM imidazole in buffer A. The 6×Histag was cleaved from the *Ec*SSADH by incubation with rTEV protease (GIBCO). Further purification was done by applying the sequential chromatographic steps of HiTrap Q ion exchange and Superdex200 size exclusion. The purified protein with three-residue cloning artifact (Gly-His-Met) at the N-terminus was concentrated to 25 mg/ml in 50 mM Tris–HCl, pH 8.0, and stored at −80 °C for crystallization trials. SDS–PAGE analysis of the purified protein showed a single band of ~51.8 kDa that corresponds to the calculated molecular weight of an *Ec*SSADH monomer.

Crystallization and structure determination of EcSSADH. *Ec*SSADH was crystallized by the sitting-drop method under conditions of 0.1 M tri-HCl, pH 7.5, and 17% PEG 2 K at 22 °C for 3 days, and crystals reached their maximal sizes in about 7 days with dimensions of approximately 0.3 × 0.2 × 0.2 mm. For data collection, 20% (w/v) glycerol was added to the crystallizing precipitant as a cryoprotectant and the crystals were immediately placed in a −173 °C nitrogen-gas stream. X-ray diffraction data of native crystals were collected at a resolution of 1.4 Å at the 6C1 beamline of the Pohang Accelerator Laboratory (PAL, Korea) using a QUANTUM 210 CCD detector (San Diego, CA, USA). The data were then indexed, integrated, and scaled using the HKL2000 suite [20]. The crystals belonged to the space group $P2_1$, with the unit cell parameters $a = 84.62$, $b = 85.43$, $c = 128.54$ Å and $\beta = 94.39°$. With four *Ec*SSADH molecules in the asymmetric unit, the crystal volume per unit of protein weight was 2.24 $Å^3\ Da^{-1}$, corresponding to a solvent content of 45.02% [21]. The structure was determined by molecular replacement with the CCP4 version of MOLREP [22] using the structure of human SSADH (PDB code 2w8o) as a search model. Model building was performed using the program Coot [23] and refinement was performed with CCP4 Refmac5 [24] and CNS [25]. The X-ray diffraction and structure refinement statistics are summarized in Table 1. The atomic coordinate and structure factor will be deposited in the Protein Data Bank.

SSADH activity assay. The spectrophotometric method was used to assay *Ec*SSADH activity. The rate of reduction of $NADP^+$ to NADPH (extinction coefficient of 6.22 mM^{-1}/cm) was measured by monitoring the increase in absorbance at 340 nm. The reaction mixture contains 100 mM sodium potassium phosphate, pH 8.5, 50 μM SSA and 200 μM $NADP^+$. The reaction was performed at room temperature for 5 min. One unit of enzyme activity was defined as the amount of enzyme catalyzing the production of 1 mmol of NADPH per mg protein/min. To investigate how *Ec*SSADH senses ROS, fully reduced *Ec*SSADH WT and C289S mutant were treated with various concentrations of H_2O_2 for 1 h before the enzyme–buffer assay mixture was added; reactions were terminated by adding 5 mM L-methionine. To switch the environment to a reduced condition, 10 mM DTT was added to H_2O_2-treated proteins, and allowed to incubate for 10 min. All incubations were performed at room temperature.

Table 1
Data collection and refinement statistics of *Ec*SSADH.

Data collection	
Space group	$P2_1$
Cell dimensions	
a, *b*, *c* (Å)	84.62, 85.43, 128.54
α, β, γ (°)	90.00, 94.39, 90.00
Resolution (Å)[a]	30.0–1.4 (1.45–1.4)[a]
R_{sym}[b]	5.1 (30.6)[a]
$I/\sigma(I)$	32.4 (2.7)[a]
Completeness (%)	98.2 (95.2)[a]
Redundancy	5.6
Refinement	
Resolution (Å)	30–1.4
No. of reflections	350,759
R_{work}[c]/R_{free}	17.9/20.1
No. atoms	
Protein	14,610
Water	1754
No. molecules	
Glycerol	6
R.m.s deviations	
Bond lengths (Å)	0.008
Bond angles (°)	1.174
B-factor (Å^2)	15.80

[a] The numbers in parentheses are statistics from the highest resolution shell.
[b] $R_{sym} = \Sigma\ |I_{obs} - I_{avg}|/I_{obs}$, where I_{obs} is the observed intensity of individual reflection and I_{avg} is an average over symmetry equivalents.
[c] $R_{work} = \Sigma\ ||F_o| - |F_c||/\Sigma\ |F_o|$, where $|F_o|$ and $|F_c|$ are the observed and calculated structure factor amplitudes, respectively. R_{free} was calculated with 5% of the data.

Results and discussion

Crystal structure of EcSSADH

To address the structural basis for the catalytic and regulatory mechanisms of bacterial SSADH, we determined the 1.4 Å crystal structure of full length *Ec*SSADH. The structure of *Ec*SSADH reveals that four monomers are present in the asymmetric unit of our present structure, forming a biological homotetramer which is observed in human SSADH as well as other members of the ALDH family. The overall structure of *Ec*SSADH shares the general fold of ALDH classes 1 and 2 [26,27]. The *Ec*SSADH monomer is composed of three domains; an N-terminal NAD(P)-binding domain (residues 1–125, 148–256, and 457–472), a catalytic domain (residues 257–456), and an oligomerization domain (residues 126–147 and 473–482) (Fig. 1A and B). As expected from the high amino acid sequence similarity between *Ec*SSADH and human SSADH, the structure of *Ec*SSADH closely resembles the reduced form of human SSADH with R.m.s. deviation of 0.73 Å. The NAD(P)-binding and catalytic domains are α/β in structure, whereas the oligomerization domain contains three-stranded antiparallel β-sheets. The catalytic residues of human SSADH (Cys340 and Glu306) are conserved in *Ec*SSADH and superimpose well with those of *Ec*SSADH (Cys289 and Glu255, respectively), implying that *Ec*SSADH might have the same reaction mechanism as human SSADH (Fig. 1C). The Cys289 residue acts as a nucleophile to attack an aldehyde group of SSA, and the Glu255 residue is used as a general base. Moreover, the substrate binding mode of *Ec*SSADH seems to be identical to that of human SSADH, because the Arg213, Arg334, and Ser498 residues involved in SSA binding in human SSADH are conserved and located at the similar positions in *Ec*SSADH (Arg165, Arg283, and Ser446, respectively) (Fig 1C).

Structural comparison between EcSSADH and human SSADH under oxidized conditions

In the previous study, our group revealed that human SSADH is regulated by a 'redox-switch modulation'. The catalytic loop of human SSADH undergoes large structural changes depending on the redox status of the environment, which is mediated by reversible disulfide bond formation between a catalytic Cys340 residue and an adjacent Cys342 residue located on the loop. The structural

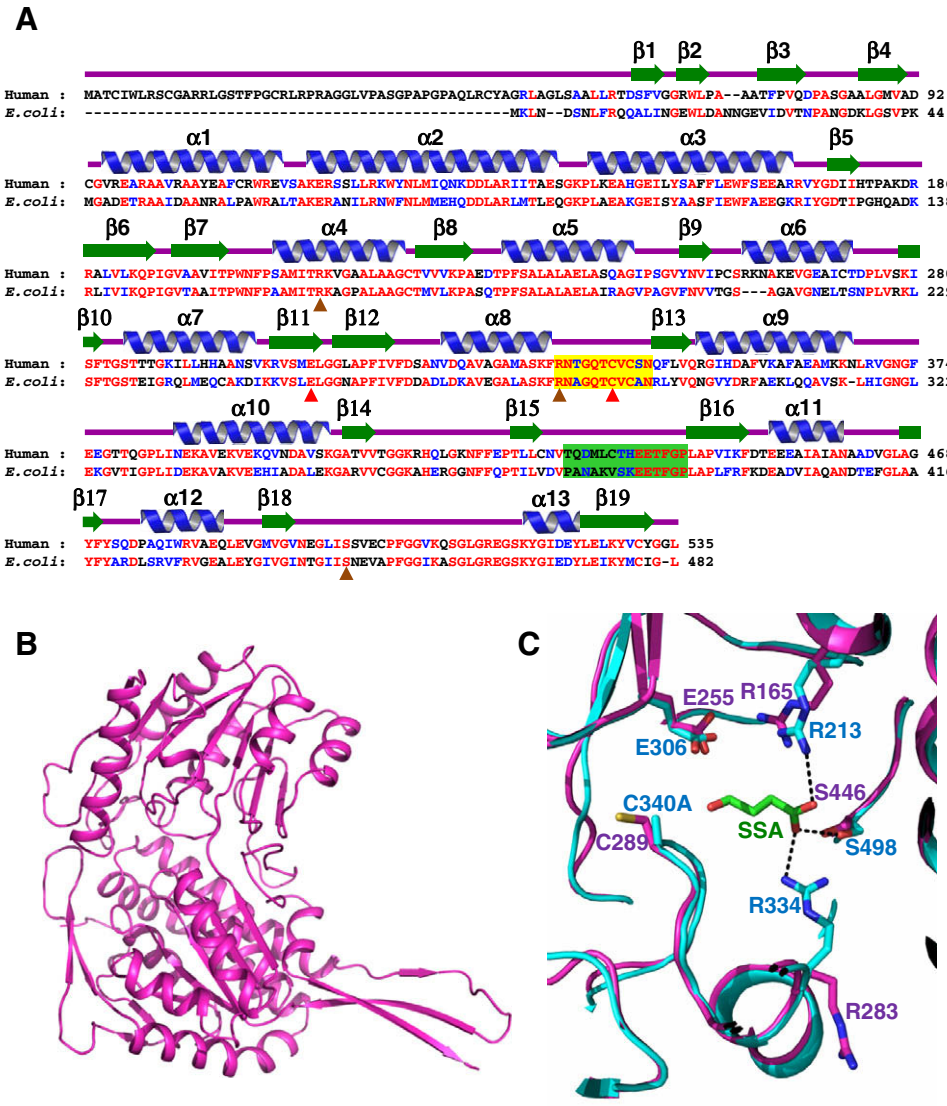

Fig. 1. Crystal structure of *Ec*SSADH. (A) Alignment of amino acid sequences of *Ec*SSADH and human SSADH. Secondary structure elements are drawn on the basis of *Ec*SSADH structure and shown with a green arrow (β-sheet) and blue helix (α-helix) and labeled. The catalytic loop region and the connecting loop (β15–β16) are shown in yellow boxes and green boxes, respectively. Residues involved in enzyme catalysis and SSA binding are indicated by red-colored and brown-colored triangles, respectively. (B) Monomeric structure of *Ec*SSADH. A monomeric protein is shown in a ribbon representation. (C) Active site of *Ec*SSADH. The active site of *Ec*SSADH is compared with that of human SSADH. *Ec*SSADH and human SSADH are shown in ribbon representations in magenta and cyan, respectively. Residues involved in enzymatic catalysis and SSA binding in *Ec*SSADH are shown in a stick model and labeled with magenta, and those in human SSADH are labeled with cyan. SSA bound in human SSADH is shown in a stick model in green, and hydrogen bonds between SSA and residues of human SSADH are drawn with black dotted lines. (For interpretation of the references to color in this figure legend, the reader is referred to the web version of this article.)

changes on the loop lead to inactivation of the enzyme, not only by oxidizing the catalytic Cys340 residue but also by blocking the binding pockets of both SSA and NAD [16]. However, in *Ec*SSADH expected conformational changes, such as a disulfide bond formation between a catalytic Cys289 residue and a neighboring Cys291 residue and subsequent structural changes on the catalytic loop were not observed under oxidized conditions (Fig. 2A). The structure of *Ec*SSADH under oxidized conditions instead shows the same conformation as the reduced form of human SSADH, where the substrate and cofactor binding pockets are open to receive SSA and NAD, respectively. The structural observation of *Ec*SSADH under oxidized conditions raises the possibility that, unlike human SSADH, *Ec*SSADH might be non-redox regulated.

Non-redox regulation of EcSSADH

In order to confirm that the catalytic loop of *Ec*SSADH does not undergo structural changes upon changes in environmental redox status, and that the protein is not regulated via 'redox-switch modulation', we examined the susceptibility of the enzyme to hydrogen peroxide (H_2O_2) and activity recovery by a reducing agent, using recombinant protein from wild-type and the C291S mutant. When the wild-type and the C291S mutant proteins were treated with various concentrations of H_2O_2, both showed almost complete loss of activity in the presence of over 100 μM H_2O_2 (Fig. 2B). When the environment was switched to a reduced state by the addition of 10 mM DTT, the activities of both the wild-type and the mutant *Ec*SSADH dramatically decreased upon the increase in H_2O_2 concentration (Fig. 2B). The results are remarkably different from observations of human SSADH, which showed that the activity of wild-type SSADH was almost completely recovered by the addition of 10 mM DTT, whereas the activity recovery of the C342A mutant dramatically decreased upon the increase in H_2O_2 concentration [16]. The differences in activity recovery between *Ec*SSADH and human SSADH indicate that *Ec*SSADH is permanently inactivated by the oxidation of the catalytic Cys291 to sulfonic or sulfinic acids

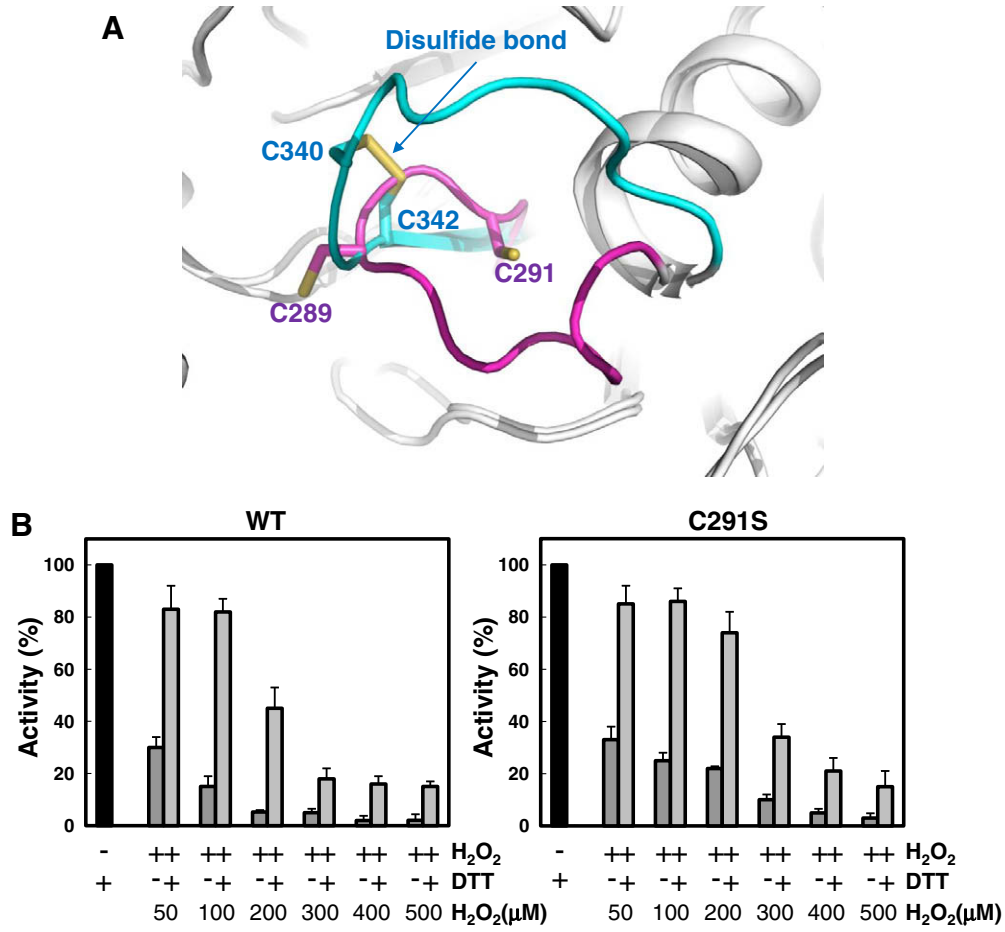

Fig. 2. Non-redox regulation of *Ec*SSADH. (A) Structural comparison between the oxidized form of *Ec*SSADH and that of human SSADH. *Ec*SSADH and human SSADH are shown in ribbon representation in gray. The catalytic loops of *Ec*SSADH and human SSADH are shown in magenta and cyan, respectively. (B) Redox change experiments. To investigate how *Ec*SSADH senses ROS, wild-type (WT) and C291S mutant proteins were treated with various concentrations of H_2O_2 in vitro and SSADH activities were measured. We then added 10 mM DTT to switch the environment to a reduced state, and compared the activity recovery between the two different forms of SSADH.

that cannot be reduced by a reducing agent, while human SSADH is protected by forming a disulfide bond between Cys340 and Cys342 under oxidative stress. This confirms that, unlike human SSADH, *Ec*SSADH does not undergo disulfide bond-mediated structural changes upon changes in environmental redox status, and that the protein is not regulated via 'redox-switch modulation'.

Comparison in catalytic dynamics between EcSSADH and human SSADH

As described above, *Ec*SSADH shares 54% amino acid sequence identity with human SSADH, and overall structures of these two proteins are almost identical. Moreover, the amino acid sequences composing the catalytic loop of *Ec*SSADH (RNAGQTCVCAN, residues 283–293) are homologous to those of human SSADH (RNTGQTCVCSN, residues 334–344) (Fig 1). However, the catalytic loop of *Ec*SSADH is more rigid compared to that of human SSADH. Interestingly, in human SSADH that is known to have a 'dynamic catalytic loop', the average *b*-factor of the catalytic loop is 1.8 times higher than that of the whole polypeptide (Fig 3A). However, similar to the static catalytic loops of other ALDHs, the catalytic loop of *Ec*SSADH has an average *b*-factor only 1.1 times higher than that of the whole polypeptide (Fig. 3A). In fact, the interactions between the catalytic loop and the remainder of the protein in *Ec*SSADH are somewhat different from those of human SSADH. In particular, the conformation of the connecting loop (β15–β16) (PANAKVSKEETFGP, residues 377–390) of *Ec*SSADH is quite different from that of human SSADH (TQDMICTHEETFGP, residues 325–338) with rms deviation of 2.59 Å (Fig 3B). The difference in connecting loop conformation causes the formation of a water molecule-mediated hydrogen bond network, which occurs only in *Ec*SSADH and not in human SSADH (Fig 3B), leading the catalytic loop of *Ec*SSADH to be more rigid compared to that of human SSADH. These structural observations confirm that the catalytic loop of *Ec*SSADH is structurally static, and that the protein might hardly undergo structural changes at all upon changes in environmental redox status.

Conclusions

Our results reveal that, unlike human SSADH, *Ec*SSADH does not undergo structural changes upon changes in environmental redox status, and therefore is non-redox regulated. We also reveal that the non-dynamic nature of the catalytic loop of *Ec*SSADH might be derived from the tight interaction between the catalytic loop and the surrounding environment of the loop. *Ec*SSADH is located at the cytosol in *E. col* while human SSADH is known to be located at the mitochondrial matrix, where relatively more oxidizing conditions are maintained compared with the cytosol [28]. Moreover, in *E. coli* the GABA shunt is proposed to function to utilize GABA as the sole nitrogen source, while in the human brain GABA is used as the most important inhibitory neurotransmitter, and its cellular

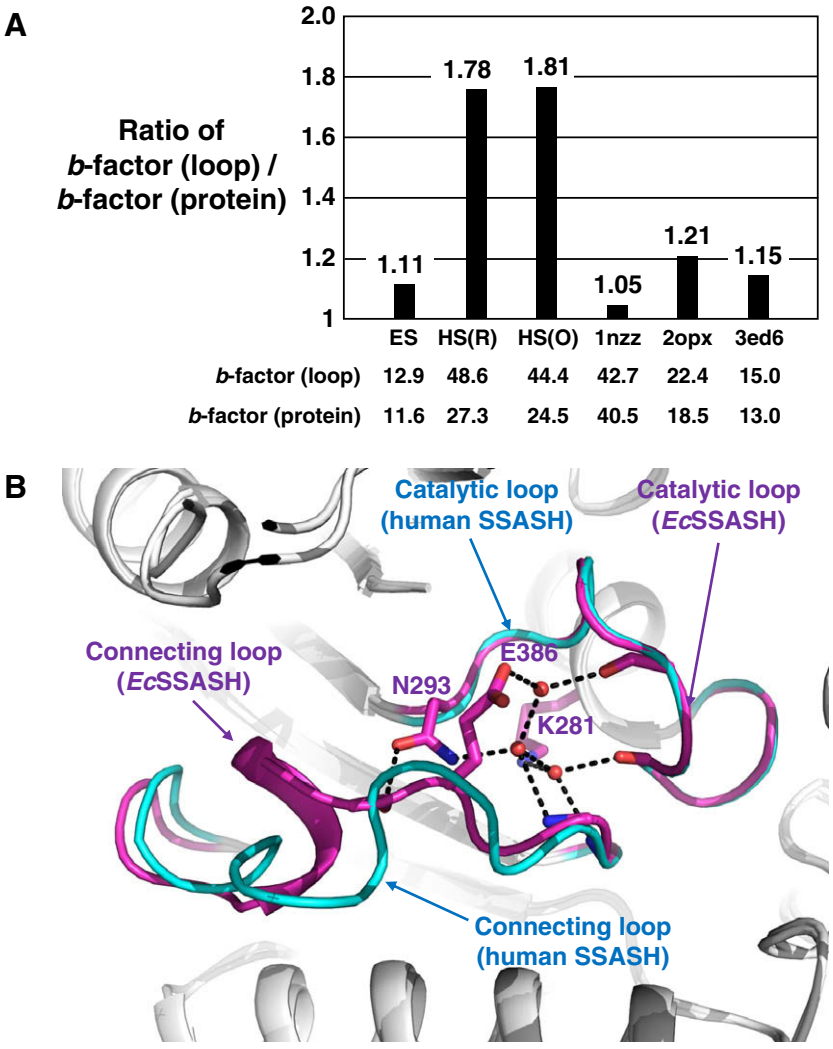

Fig. 3. Comparisons of catalytic loop dynamics. (A) Comparison of the average *b*-factors of the catalytic loop and the whole polypeptide. The average *b* -factor between the catalytic loop region and the whole polypeptide are compared. ES, HS(R) and HS(O) represent *Ec*SSADH, the reduced form of human SSADH, and the oxidized form of human SSADH, respectively. 1nzz, 2opx, and 3ed6 are pdb codes for Human mitochondrial aldehyde dehydrogenase, *E. coli* Lactaldehyde Dehydrogenase and *Staphylococcus aureus* betaine aldehyde dehydrogenase, respectively. (B) Stabilization of the catalytic loop. *Ec*SSADH and human SSADH are shown in ribbon representations in gray. The catalytic loop and the connecting loop (β15–β16) of *Ec*SSADH are shown in magenta, and those of human SSADH are in cyan. Three water molecules involved in a hydrogen bond network for the stabilization of the *Ec*SSADH catalytic loop are shown in red spheres; hydrogen bonds that form between the catalytic loop and the connecting loop (β15–β16) are shown in black dotted lines. (For interpretation of the references to color in this figure legend, the reader is referred to the web version of this article.)

concentration needs to be elaborately regulated. We suspect that these differences, in localization of the proteins and the cellular function of the GABA shunt, result in the difference in regulatory mechanism between *Ec*SSADH and human SSADH. In fact, SSADH from *Drosophila melanogaster* (*Dm*SSADH) contains Ser313 instead of a cysteine residue at the corresponding positions of Cys291 and Cys342 in *Ec*SSADH and human SSADH, respectively, indicating that the catalytic Cys311 of *Dm*SSADH lacks a partner cysteine residue for a disulfide bond formation, implying that the protein is fundamentally non-redox regulated. Taken together, we propose that the presence of a redox or non-redox regulatory mechanism for SSADH is organism-dependent, and that the choice of regulatory mechanism might be determined by the cellular localization and function of the protein in its organism.

Acknowledgments

This work was supported by the National Research Foundation of Korea Grant funded by the Korean Government(MEST)" (NRF-2009-C1AAA001-2009093479), and also supported by the 21C Frontier Microbial Genomics and Application Center Program, Ministry of Education, Science and Technology (MEST), Republic of Korea.

References

[1] P.L. Pearl, K.M. Gibson, M.T. Acosta, L.G. Vezina, W.H. Theodore, M.A. Rogawski, E.J. Novotny, A. Gropman, J.A. Conry, G.T. Berry, M. Tuchman, Clinical spectrum of succinic semialdehyde dehydrogenase deficiency, Neurology 60 (2003) 1413–1417.
[2] C.G. Wong, T. Bottiglieri, O.C. Snead, GABA, gamma-hydroxybutyric acid, and neurological disease, Ann. Neurol. 54 (Suppl. 6) (2003) S3–S12.
[3] P. Blasi, P.P. Boyl, M. Ledda, A. Novelletto, K.M. Gibson, C. Jakobs, B. Hogema, S. Akaboshi, F. Loreni, P. Malspina, Structure of human succinic semialdehyde dehydrogenase gene: identification of promoter region and alternatively processed isoforms, Mol. Genet. Metab. 76 (2002) 348–362.
[4] G. Fenalti, R.H. Law, A.M. Buckle, C. Langendorf, K. Tuck, C.J. Rosado, N.G. Faux, K. Mahmood, C.S. Hampe, J.P. Banga, M. Wilce, J. Schmidberger, J. Rossjohn, O. El-Kabbani, R.N. Pike, A.I. Smith, I.R. Mackay, M.J. Rowley, J.C. Whisstock, GABA production by glutamic acid decarboxylase is regulated by a dynamic catalytic loop, Nat. Struc. Mol. Biol. 14 (2007) 280–286.
[5] T.G. Porter, D.C. Spink, S.B. Martin, D.L. Martin, Transaminations catalysed by brain glutamate decarboxylase, Biochem. J. 231 (1985) 705–712.
[6] G. Battaglioli, H. Liu, D.L. Martin, Kinetic differences between the isoforms of glutamate decarboxylase: implications for the regulation of GABA synthesis, J. Neurochem. 86 (2003) 879–887.

[7] P. Storici, D. De Biase, F. Bossa, S. Bruno, A. Mozzarelli, C. Peneff, R.B. Silverman, T. Schirmer, Structures of gamma-aminobutyric acid (GABA) aminotransferase, a pyridoxal 5′-phosphate, and [2Fe–2S] cluster-containing enzyme, complexed with gamma–ethynyl–GABA and the antiepilepsy drug vigabatrin, J. Biol. Chem. 279 (2004) 363–373.
[8] M. Maitre, The gamma-hydroxybutyrate signaling system in the brain: organization and functional implications, Prog. Neurobiol. 51 (1997) 337–361.
[9] V.P. Kelly, P.J. Sherratt, D.H. Crouch, J.D. Hayes, Novel homodimeric and heterodimeric rat gamma-hydroxybutyrate synthases that associate with the Golgi apparatus define a distinct subclass of aldo-keto reductase 7 family proteins, Biochem. J. 366 (2002) 847–861.
[10] K.M. Gibson, G.F. Hoffmann, A.K. Hodson, T. Bottiglieri, C. Jakobs, 4-Hydroxybutyric acid and the clinical phenotype of succinic semialdehyde dehydrogenase deficiency, an inborn error of GABA metabolism, Neuropediatrics 29 (1998) 14–22.
[11] B.M. Hogema, M. Gupta, H. Senephansiri, T.G. Burlingame, M. Taylor, C. Jakobs, R.B. Schutgens, W. Froestl, O.C. Snead, R. Diaz-Arrastia, T. Bottiglieri, M. Grompe, K.M. Gibson, Pharmacologic rescue of lethal seizures in mice deficient in succinate semialdehyde dehydrogenase, Nat. Genet. 29 (2001) 212–216.
[12] K.M. Gibson, D.S. Schor, M. Gupta, W.S. Guerand, H. Senephansiri, T.G. Burlingame, H. Bartels, B.M. Hogema, T. Bottiglieri, W. Froestl, O.C. Snead, M. Grompe, C. Jakobs, Focal neurometabolic alterations in mice deficient for succinate semialdehyde dehydrogenase, J. Neurochem. 81 (2002) 71–79.
[13] M. Gupta, R. Greven, E.E. Jansen, C. Jakobs, B.M. Hogema, W. Froestl, O.C. Snead, H. Bartels, M. Grompe, K.M. Gibson, Therapeutic intervention in mice deficient for succinate semialdehyde dehydrogenase (gamma-hydroxybutyric aciduria), J. Pharmacol. Exp. Ther. 302 (2002) 180–187.
[14] M. Gupta, B.M. Hogema, M. Grompe, T.G. Bottiglieri, A. Concas, G. Biggio, C. Sogliano, A.E. Rigamonti, P.L. Pearl, O.C. Snead, C. Jakobs, K.M. Gibson, Murine succinate semialdehyde dehydrogenase deficiency, Ann. Neurol. 54 (Suppl. 6) (2003) S81–S90.
[15] A. Latini, K. Scussiato, G. Leipnitz, K.M. Gibson, M. Wajner, Evidence for oxidative stress in tissues derived from succinate semialdehyde dehydrogeanse-deficient mice, J. Inherit. Metab. Dis. 30 (2007) 800–810.
[16] Y.G. Kim, S. Lee, O.S. Kwon, S.Y. Park, S.J. Lee, B.J. Park, K.J. Kim, Redox-switch modulation of human SSADH by dynamic catalytic loop, EMBO J. 28 (2009) 959–968.
[17] K. Bartsch, A. von Johnn-Marteville, A. Schulz, Molecular analysis of two genes of the *Escherichia coli* gab cluster: nucleotide sequence of the glutamate: succinic semialdehyde transaminase gene (gabT) and characterization of the succinic semialdehyde dehydrogenase gene (gabD), J. Bacteriol. 172 (1990) 7035–7042.
[18] E.A. Metzer, Y.S. Halpern, In vivo cloning and characterization of the gabCTDP gene cluster of *Escherichia coli* K-12, J. Bacteriol. 172 (1990) 3250–3256.
[19] E. Niegemann, A. Schulz, K. Bartsch, Molecular organization of the *Escherichia coli* gab cluster: nucleotide sequence of the structural genes gabD and gabP and expression of the GABA permease gene, Arch. Microbiol. 160 (1993) 454–460.
[20] Z. Otwinowski, W. Minor, Procession of x-ray diffraction data collected in oscillation mode, Methods Enzymol. 276 (1997) 307–326.
[21] B.W. Matthews, Solvent content of protein crystals, J. Mol. Biol. 33 (1968) 491–497.
[22] A. Vagin, A. Teplyakov, MOLREP: an automated program for molecular replacement, J. Appl. Crystallogr. 30 (1997) 1022–1025.
[23] P. Emsley, K. Cowtan, Coot: model-buiiding tools for molecular graphics, Acta Crystallogr. D: Biol. Crystallogr. 60 (2004) 2126–2132.
[24] G.N. Murshudov, A.A. Vagin, E.J. Dodson, Refinement of macromolecular structures by the maximum-likelihood method, Acta Crystallogr. D: Biol. Crystallogr. 53 (1997) 240–255.
[25] A.T. Brünger, P.D. Adams, G.M. Clore, W.L. DeLano, P. Gros, R.W. Grosse-Kunstleve, J.S. Jiang, J. Kuszewski, M. Nilges, N.S. Pannu, R.J. Read, L.M. Rice, T. Simonson, G.L. Warren, Crystallography & NMR system: a new software suite for macromolecular structure determination, Acta Crystallogr. D: Biol. Crystallogr. 54 (1998) 905–921.
[26] C.G. Steinmetz, P. Xie, H. Weiner, T.D. Hurley, Structure of mitochondrial aldehyde dehydrogenase: the genetic component of ethanol aversion, Structure 5 (1997) 701–711.
[27] S.A. Moore, H.M. Baker, T.J. Blythe, K.E. Kitson, T.M. Kitson, E.N. Baker, Sheep liver cytosolic aldehyde dehydrogenase: the structure reveals the basis for the retinal specificity of class 1 aldehyde dehydrogenases, Structure 6 (1998) 1541–1551.
[28] J. Hu, L. Dong, C.E. Outten, The redox environment in the mitochondrial intermembrane space is maintained separately from the cytosol and matrix, J. Biol. Chem. 283 (2008) 29126–29134.